International Journal of Biological Macromolecules 253 (2023) 127318

Contents lists available at ScienceDirect

International Journal of Biological Macromolecules

journal homepage: www.elsevier.com/locate/ijbiomac

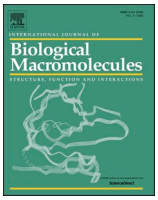

Characterization of active films of chitosan containing nettle *Urtica dioica* L. extract: Spectral and water properties, microstructure, and antioxidant activity

María Flórez, Patricia Cazón *, Manuel Vázquez

Department of Analytical Chemistry, Faculty of Veterinary, Campus Terra, University of Santiago de Compostela, 27002 Lugo, Spain

ARTICLE INFO

Keywords:
Nettle extract
Chitosan
Active packaging

ABSTRACT

Chitosan films enriched with aqueous nettle extract (*Urtica dioica* L.) were evaluated by measuring their solubility, equilibrium moisture, water vapor permeability, spectral and antioxidant properties, and microstructure. Nettle extract showed a significant effect on the analyzed film properties. The addition of nettle extract manifested a sharp decrease in water vapor permeability, decreasing from $5.64 \cdot 10^{-11}$ to $2.22 \cdot 10^{-11}$ g/m·s·Pa. The chitosan- nettle extract films exhibited a high free-radical scavenging activity against 2,2-diphenyl-1-picrylhydrazyl (DPPH) and 2,2′-azino-bis (3-ethylbenzothiazoline-6-sulfonic acid) (ABTS). Incorporation of nettle extract into the chitosan matrix was successfully carried out to obtain antioxidant films. The results obtained showed that the incorporation of nettle extract allowed obtaining chitosan films with antioxidant properties, including a total phenolic content up to 1.57 mg GAE/g film. Furthermore, the films with nettle extract boast an UV shielding ability with transmittance values close to zero in the UV region and a water solubility up to 1 %. The inherent biodegradability is also a strong advantage of the developed active films.

1. Introduction

A wide variety of biopolymers including polysaccharides have been studied for developing films for food applications. These biopolymers are compatible with plasticizers, plant extracts and other materials, resulting in high presence of hydroxyl, amino, carbonyl and polar groups when the film is formed. This hydrogen bond network structure formed between the polar groups allows the film to adopt good mechanical and barrier properties [1]. The study of the application of chitosan-based films to extend the shelf life of perishable foods has become widespread due to their biodegradability, origin from renewable sources and their antimicrobial properties [2]. These films can become active packaging when components capable of enhancing the antioxidant and/or antimicrobial action are incorporated, promoting a protective capacity [3,4].

The development of packaging systems with antioxidant function is essential for food protection. Textural changes, discoloration, and the appearance of off-flavors in foods are effects related to the presence of oxygen in the environment [5]. The development and use of active packaging systems with antioxidant capabilities is a promising alternative to increase the stability of oxidation-sensitive foods [6].

A wide variety of plant extracts have been studied in relation to their effects on the techno-functional characteristics of food packaging, such as *Pistacia terebinthus* [7], *Santalum album* [8], and *Nephelium lappaceum* [9]. The use of natural antioxidants, in particular polyphenols, obtained from plants and agricultural by-products is one of the current topics in food packaging research [6].

Urtica, commonly known as nettle, is a plant belonging to the Urticaceae family characterized by its serrated leaves [10]. These leaves have a lipid profile composed of fatty acids such as α-linolenic acid, palmitic acid, and cis-9,12-linoleic acid. It also contains, although to a lesser extent, n-3 and n-6 fatty acids. Its mineral profile is constituted by micro and macroelements such as Na, K, Ca, Mg, Fe and Mn [11,12]. Nettle extract (NE) are a useful natural source of polyphenols, pigments, and bioactive chemicals [13]. There are several species of nettle: *Urtica dioica* L., *Urtica membranacea* Poir, and *Urtica urens* L. Nevertheless, *Urtica dioica* L. has the highest concentration of polyphenols [14]. Polyphenols such as chlorogenic, ferulic, and chicoric acid, and flavonoids such as luteolin or quercetin-3-glucoside are identified in the nettle extract [13]. The antioxidant properties of this extract depended on the time and solvent used, as well as the time of harvesting, the sun exposure, or the soil in which it has grown [12,15].

* Corresponding author.
E-mail addresses: patricia.cazon.diaz@usc.es (P. Cazón), manuel.vazquez@usc.es (M. Vázquez).

https://doi.org/10.1016/j.ijbiomac.2023.127318
Received 26 June 2023; Received in revised form 5 October 2023; Accepted 6 October 2023
Available online 7 October 2023

Table 1
Chitosan (Ch) films 1 % (w/w) with different glycerol (Gly) and nettle extract (NE). The number in the film sample shows the % (w/w) of that compound.

Film samples	Glycerol	Nettle extract
	% (w/v)	% (v/v)
Ch_Gly0	0	0
Ch_Gly0_NE12.5	0	12.5
Ch_Gly0_NE25	0	25
Ch_Gly0.25	0.25	0
Ch_Gly0.25_NE12.5	0.25	12.5
Ch_Gly0.25_NE25	0.25	25
Ch_Gly0.5	0.5	0
Ch_Gly0.5_ NE12.5	0.5	12.5
Ch_Gly0.5_ NE25	0.5	25

In a prior study [16], the antioxidative attributes of chitosan films infused with NE were examined, both in their unconstrained state and when integrated into nanoliposomes. Moreover, films with heightened activity were developed by combining chitosan and hydroxypropyl methylcellulose, further supplemented with NE [17]. However, it is worth noting that the comprehensive investigation of the physico-chemical and operational traits of unalloyed chitosan films incorporated with NE remains an unexplored area within the existing literature. Nettle is a highly available and low-cost plant worldwide. Therefore, it is interesting to give it new applications. The objective of this study was to develop an active chitosan-based food packaging film with NE extract (Ch_NE). The effect of NE at different ratios on the optical, solubility, water retention, equilibrium moisture content, water vapor permeability (WVP) and antioxidant properties of the films were analyzed. Scanning electron microscope (SEM) and Fourier transform infrared spectroscopy (FT-IR) were carried out to evaluate the surface morphology and compatibility of the mixture.

2. Material and methods

2.1. Materials

Chitosan (M_w 100,000–300,000 and CAS number 9012-76-4) was purchased from Acros organics (Geel, Belgium). Acetic acid (CAS number 64-19-7) and glycerol (CAS number 56-81-5) were provided by Scharlau Microbiology (Barcelona, Spain). *Urtica dioica* was collected (43°32′51.659″N 6°31′17.548″W) from Luarca (Asturias, Spain) from September to October 2022. 2,2-diphenyl-1-picrylhydrazyl radicals (DPPH) and 2,2′-azino-bis (3-ethylbenzothiazoline-6-sulfonic acid) (ABTS) were provided by Alfa Aesar (Haverhill, MA, USA). Folin-Ciocalteu phenol reagent was provided by Panreac (Barcelona, Spain).

2.2. Preparation of plant extract

The nettle plant was cleaned and defoliated to obtain healthy leaves of similar size. The nettle leaves were dried in a Model 3500 dehydrator (Excalibur® Food, Sacramento, CA, USA) at 45 °C for 24 h to remove the water content. Afterwards, the leaves were crushed and ground into powder with an electric grinder. The nettle powder was stored in high density polyethylene (HDPE) wide mouth cylindrical flasks with cap and shutter (Duchess type) at room temperature.

The aqueous nettle extract was obtained according to the optimized conditions previously studied as described elsewhere [15]. The nettle extract was filtered with Whatman no. 1 filter paper using a funnel to remove any solid residues present in the aqueous extract. The extract was refrigerated for 24 h to precipitate any residue. Thereupon it was filtered with a funnel and finally centrifuged at 9000 rpm and 5 °C for 20 min. The extract was stored in darkness and refrigerated at 5 °C.

2.3. Preparation of films

Chitosan films were made by dissolving 2 % (w/w) chitosan in an aqueous solution of 1 % (w/v) acetic acid (Table 1). The stock solution was kept stirred overnight at room temperature. Glycerol at a concentration from 0, 0.25 and 0.5 % (w/v) was added as a plasticizer. Consecutively, NE was added to chitosan solution until a final concentration of NE in the range of 0, 12.5 and 25 % (v/v) and chitosan 1 % (w/w) by homogenizing at 15000 rpm for 2 min (Ultra Turrax®, IKA, Staufen, Germany). The bubbles of the filmogenic solution were removed by ultrasonic bath for 15 min.

In a Petri plate of 210 diameter, 40 ml of the resulting film-forming solution was poured. Depending on the test, the films were cut to a specified size and conditioned for 5 days. The thickness (mm) was measured at five random locations using a Thickness Meter ET115S (Etari GmbH, Stuttgart, Germany).

2.4. Scanning electron microscope (SEM) and Fourier transform infrared spectroscopy (FT-IR)

The morphology of the Ch_NE films was examined and characterized through SEM pictures. A high-vacuum microscope (JEOL JSM-6360LV, Jeol Ltd, Tokyo, Japan) working at an accelerating voltage of 20 kV was used to photograph dry and gold-coated samples. Samples were adhered to slides using conductive double-sided carbon tape.

FT-IR 6800 (Jasco Inc., Japan) was used to determine the presence of certain chemical groups and their cross-linking in the films. The samples were conditioned at 65 ± 2 % relative humidity and 21 ± 1 °C for 48 h. FT-IR spectra were recorded in the range (400–4000) cm^{-1} with a spectral resolution of 4 cm^{-1}.

2.5. Water solubility, equilibrium moisture, water vapor permeability and water retention

The water solubility of the film samples was assessed using the gravimetric method of immersion in a predetermined volume of distilled water, as previously described [18]. For this purpose, a rectangular sample of 3 cm side previously dried at 105 °C in an oven was weighed using a precision balance. The sample was then immersed for 24 h in 100 ml of distilled water at 25 °C and under agitation. After 24 h, the sample was dried again at 105 °C, and the final weight was taken. The solubility of the films was calculated by the difference in weights of the initial sample and the final sample. The equilibrium moisture content (EMC) was calculated in a similar manner. Previously samples conditioned at 33 % relative humidity (% RH) were weighed at 33%RH and then dried at 105 °C. EMC was determined by comparing the weights of dried samples conditioned at 33 % RH [18]. Tests were carried out by triplicate.

On the other hand, the water vapor permeability (WVP) of the samples was calculated following the ASTM Standard Test Method E96 (https://www.astm.org/e0096_e0096m-22a.html) as described elsewhere [19]. WVP which it is used to quantify water vapor barrier properties, measures the amount of water that permeates per unit of area and time (g/s·m·Pa) taking into account the pressure differential and thickness of the material. For this purpose, a wide-mouth cup ($5 \cdot 10^{-3}$ m^2 area) with 100 ml of distilled water was sealed with a sample. The cup was fitted in a double-bottom permeability chamber with temperature control (30 °C) designed to be placed on an analytical balance. The design of the permeability chamber has been described in detail elsewhere [19]. The weight of the cup was recorded to the nearest $1 \cdot 10^{-4}$ g and plotted as a function of time. Each test was performed by triplicate [18].

2.6. Antioxidant and optical properties of films

The antioxidant capacity of the chitosan-NE (Ch_NE) films was

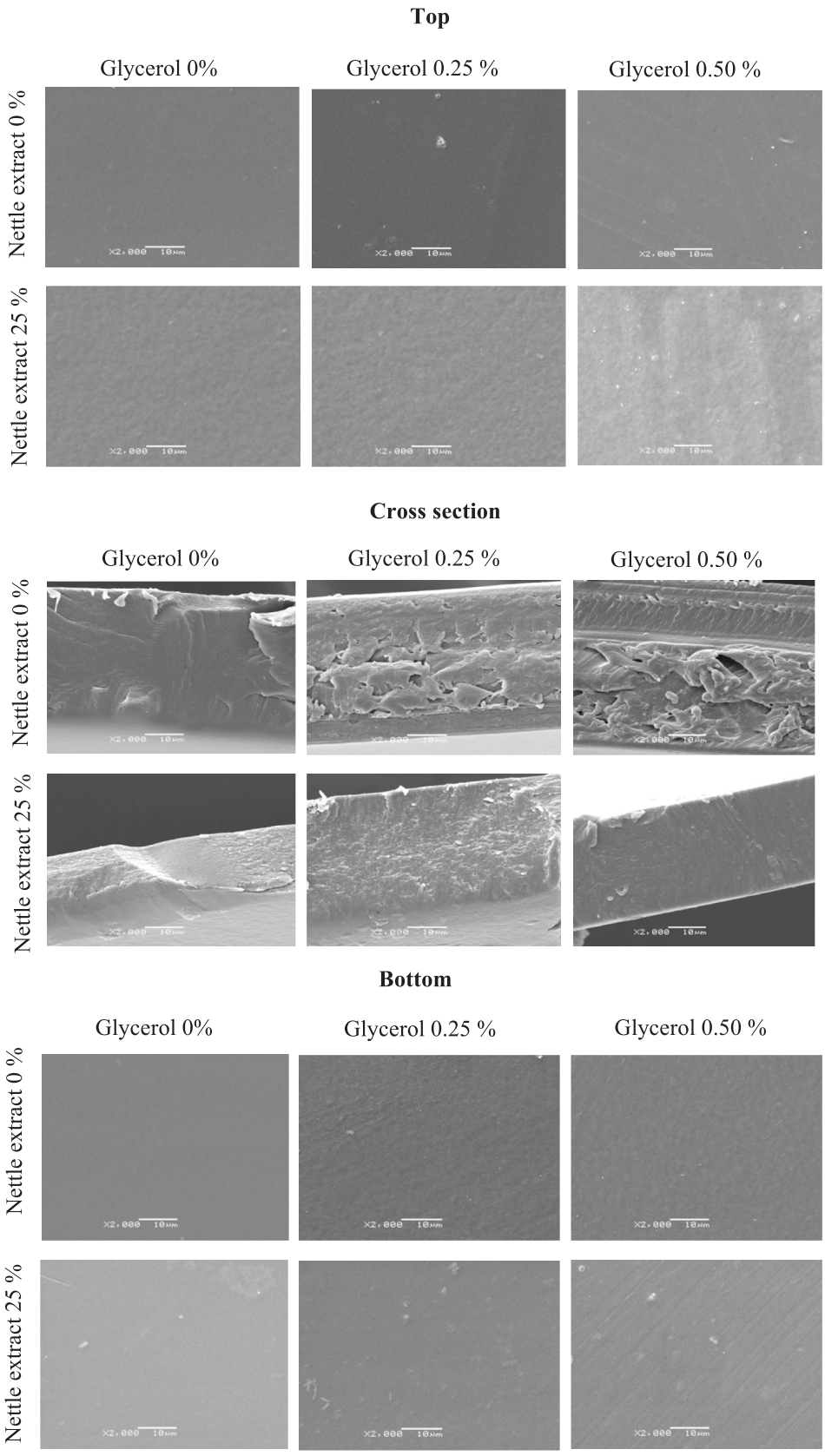

Fig. 1. Scanning electron microscopy images of the top, bottom and cross section of the pure chitosan films and chitosan-nettle films.

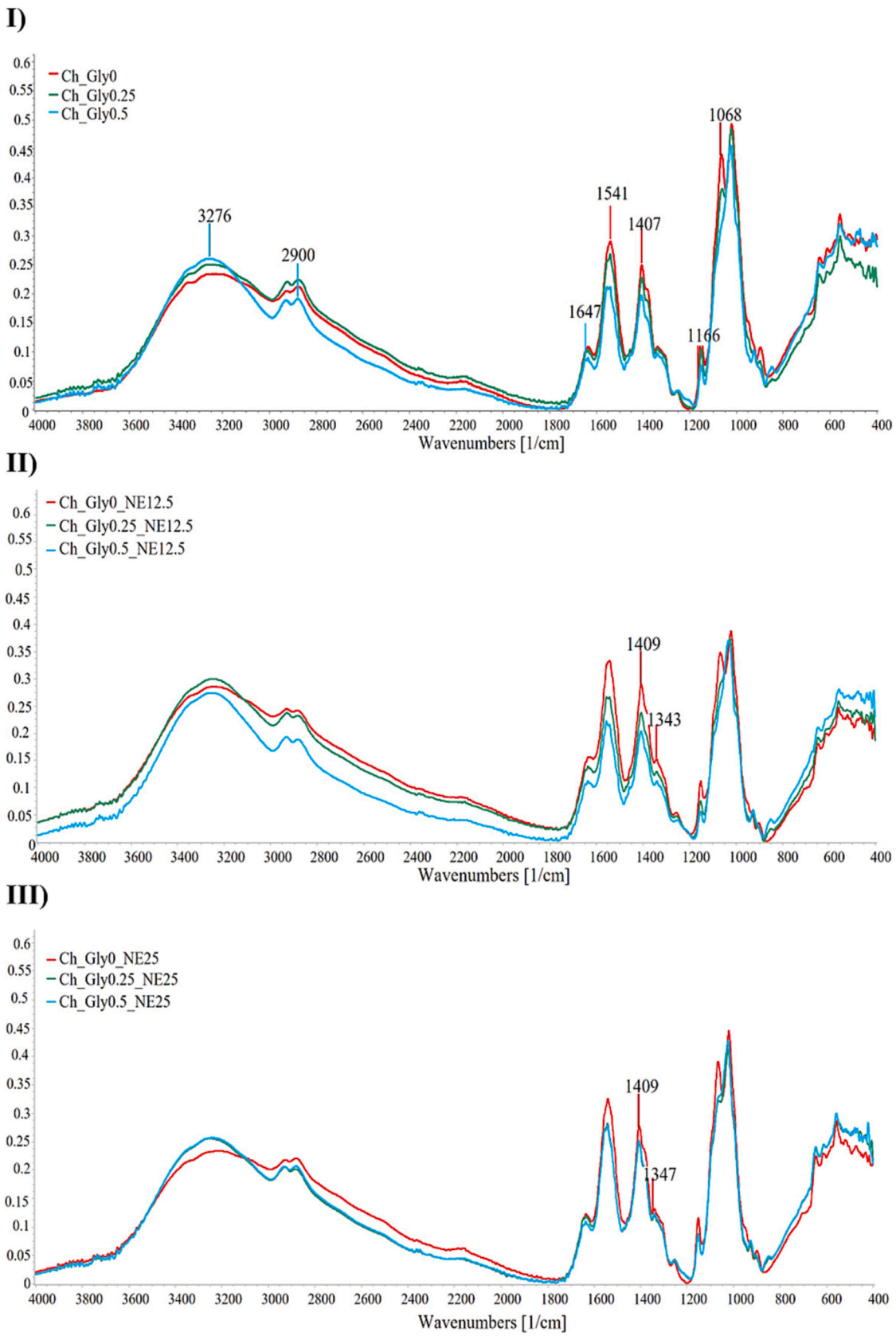

Fig. 2. FT-IR spectra of chitosan (Ch) films at different concentration of glycerol (Gly) (0, 0.25, 0.5 %) and nettle extract (NE) (0, 12.5, 25 %).

Table 2
Water properties of chitosan (Ch) films with glycerol (Gly) and nettle extract (NE). The number in the film sample shows the % (w/w) of that compound.

Film samples	Solubility (%)	Equilibrium moisture content (%)	Water vapor permeability (g/m·s·Pa)
Ch_Gly0	0.64 ± 0.17^{a}	0.98 ± 0.23^{acd}	$3.43 \cdot 10^{-11} \pm 4.81 \cdot 10^{-12a}$
Ch_Gly0_NE12.5	0.65 ± 0.37^{ac}	0.68 ± 0.23^{ac}	$4.11 \cdot 10^{-11} \pm 1.73 \cdot 10^{-11ab}$
Ch_Gly0_NE25	1.06 ± 0.16^{abc}	0.53 ± 0.09^{a}	$2.22 \cdot 10^{-11} \pm 5.02 \cdot 10^{-12a}$
Ch_Gly0.25	0.70 ± 0.10^{ac}	1.32 ± 0.44^{acd}	$3.25 \cdot 10^{-11} \pm 4.691 \cdot 10^{-12ab}$
Ch_Gly0.25_NE12.5	1.24 ± 0.19^{bc}	1.45 ± 0.32^{acd}	$3.86 \cdot 10^{-11} \pm 2 \cdot 10^{-12ab}$
Ch_Gly0.25_NE25	1.15 ± 0.05^{abc}	1.03 ± 0.51^{acd}	$3.67 \cdot 10^{-11} \pm 2.15 \cdot 10^{-12ab}$
Ch_Gly0.5	0.69 ± 0.21^{ac}	2.76 ± 0.85^{bc}	$5.53 \cdot 10^{-11} \pm 6.58 \cdot 10^{-12b}$
Ch_Gly0.5_ NE12.5	1.17 ± 0.09^{cd}	1.73 ± 0.12^{cbd}	$3.93 \cdot 10^{-11} \pm 1.20 \cdot 10^{-11ab}$
Ch_Gly0.5_NE25	1.26 ± 0.07^{bd}	2.07 ± 0.31^{d}	$5.64 \cdot 10^{-11} \pm 9.14 \cdot 10^{-11b}$

Values are expressed as mean ± standard deviation (SD). Different letters in the same column indicate significant differences ($p < 0.05$).

assessed using two different methods: 2,2-diphenyl-1-picrylhydrazyl radicals (DPPH) and 2,2′-azino-bis (3-ethylbenzothiazoline-6-sulfonic acid) (ABTS) free radical scavenging. Besides, the Folin-Ciocalteu assay was followed to calculate the total phenolic content (TPC). Using 1 g of film in 24 ml of methanol and stirring the mixture overnight in the dark, the methanolic extracts of the films were used to create the aliquots. The mixture was homogenized in vortex for 1.5 min and then it was filtered through Whatman no. 1 filter paper [20]. The radical scavenging on DPPH was examined using a UV–Vis spectrophotometer V-670 (Jasco Inc., Japan) at 515 nm, the radical cation scavenging activity of ABTS was examined at 734 nm and the total phenolics content was examined at 765 nm [21]. The results were expressed as % DPPH, % ABTS scavenging activity and gallic acid equivalents (GAE; mg GAE/g of film).

The UV–Vis spectra of the film samples were measured using a spectrophotometer V-670 (Jasco Inc., Japan), and the optical properties of the films were established as described elsewhere [18].

2.7. Statistical analysis

One-way analysis of variance (ANOVA) was used to statistically examine the results using Microsoft Excel® software. The Tukey Post Hoc test was performed to examine differences between results based on confidence intervals. The least significant difference was at $p < 0.05$. Moreover, the results obtained were analyzed using the Design Expert 11® software (Stat-Ease, Minneapolis, MN, USA). The experimental design denoted the independent variables glycerol and NE content as code variables A and B, respectively. The effect of glycerol and NE content on the dependent variables (water solubility, equilibrium moisture content, and water vapor permeability, DPPH, ABTS, total phenolic compounds, UV region transmittance, transparency, opacity and color parameters) was calculated and evaluated following a complete factorial design.

3. Results and discussion

3.1. Scanning electron microscopy (SEM) of the films

The SEM images of the top, cross-section and bottom of the films are shown in Fig. 1. The bottom SEM images are those that correspond to the face directly in contact with the Petri dish. As it is shown, the surface morphology of the chitosan film was observed to be smooth, compact, and free of any pores. This agrees with the observations in other studies [7,8]. The addition of NE allowed a homogeneous distribution without cracks or perforations. The top SEM images are those that correspond to the surface side of the film that is in contact with the environment. Like the bottom SEM images, the presence of glycerol and NE did not produce significant alteration on the morphological surface of the samples. The formation of ordered and homogeneous matrix suggested a good compatibility between chitosan and NE to form the film.

On the other hand, the absence of irregularities on the top and bottom face demonstrates that the ultrasonic bath had a positive effect by removing any air bubbles [22]. Regarding the cross-section images, pure chitosan films have a homogeneous and denser structure, whereas glycerol promoted a less close structure due to its hydrating effect. However, the presence of NE gave a denser and closer structure even in the presence of glycerol.

3.2. Fourier transform infrared spectroscopy (FT-IR)

FT-IR analysis was carried out to identify the molecular interactions between the functional groups of chitosan, glycerol and NE. Fig. 2 shows the FT-IR spectra of the pure chitosan films (Fig. 2.I), with 12.5 % NE concentration (Fig. 2.II) and with 25 % NE (Fig. 2.III) at different glycerol concentration in the range between 4000 and 400 cm^{-1}. FT-IR spectra of the samples of chitosan films with glycerol and NE at different concentrations showed characteristic bands. Firstly, the band appearing at 3256–3800 cm^{-1} is related to the stretching vibration of -NH_2 and -OH groups of chitosan [23]. The absorption peak around 3276 cm^{-1} is due to the presence of glycerol and its concentration of -OH groups. Therefore, the curve is steeper for films with a concentration of 0.5 % (blue line). The -NH stretching vibrations of chitosan are represented at this absorbance [24,25]. Furthermore, it can be determined that the addition of glycerol to the matrix affected the molecular interactions. This is observed by increasing the intensity at 3256–3800 cm^{-1} is related to the stretching vibration -OH group (Fig. 2.I). On the other hand, the peaks represented around 1600 cm^{-1} were attributed to the benzene rings of the polyphenolic compounds of the plant extract [26]. Besides that, in the 1409 cm^{-1} region, there is a noticeable peak attributed to the stretching of the -CH_2 group as well as by the contribution of aromatic bonds from nettle [7,27]. The short peak found around 1347 cm^{-1} could be attributed to the phenolic compounds present in nettle, as it is more intense in films with a higher concentration of extract [23].

The film's arrangement and interaction among its components can be discerned. The presence of glycerol and NE promoted a change and increase in absorbance at specific peaks. Similar behaviours were observed in chitosan films to which plant extracts were added, such as *Pistacia terebinthus* [7], *Berberis crataegina* [7], and *Melaleuca alternifolia* oil [22].

3.3. Evaluation of the water solubility, equilibrium moisture content, and water vapor permeability

The water solubility of the films was determined by analyzing the soluble matter of the samples. Film solubility is associated with changes in hydrogen bonds, ionization of amino or carboxyl groups, and relaxation of the film structure [28]. The calculated solubility content of the samples ranged from 0.64 to 1.26 % (Table 2). The obtained mathematical model was significant, indicating that the solubility of samples depended on their formulation.

The F-value and p-value of the model were 8.74 and 0.0167, respectively. The p-values of the model terms indicated that the linear effect of NE (B) was the only significative term (p-value < 0.05) with a strong effect on the solubility content. The effect of the glycerol

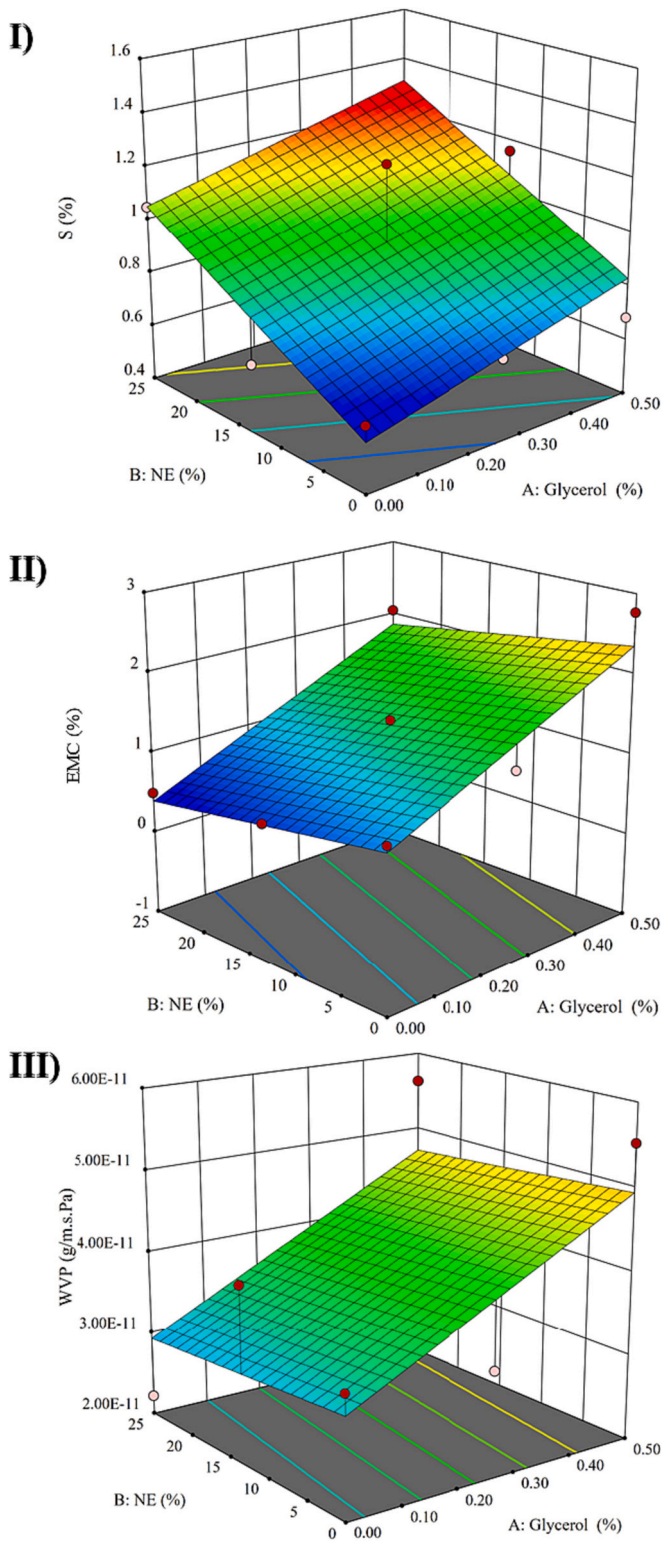

Fig. 3. Prediction of the models for the water properties of the films: I) Solubility (S), II) equilibrium moisture content (EMC) and III) water vapor permeability (WVP). NE is nettle extract.

concentration (A) was not significant (p-value > 0.05) (Table S1). The fit statistics results (Table S2) indicated a r^2 of 0.74. The adjusted r^2 was utilized to assess the goodness-of-fit of regression models with varying numbers of independent variables. The predicted r^2 indicates the model's ability to forecast a response value. For a reasonable concurrence, the gap between the adjusted r^2 and predicted r^2 should be <0.20. In this case, the predicted r^2 (0.53) was in reasonable agreement with the adjusted r^2 (0.65). To assess the precision, the range of the expected values at the design points is compared with the average prediction error using a signal-to-noise ratio. If the ratio exceeds 4, it indicates sufficient model discrimination. In the solubility property, the adequate precision obtained was 8.00, which implies an adequate signal.

Eq. (1) predicts the solubility response (S) in terms of actual factors of glycerol and NE concentration.

$$S\ (\%) = 0.58 + 0.51 \cdot Glycerol\ (\%) + 0.02 \cdot NE\ (\%) \quad (1)$$

Fig. 3.I shows the calculated dependence of the solubility of chitosan films given by Eq. (1). The solubility of Ch_NE film got slightly enhanced up to 1.26 % as compared to 0.64 % for pure chitosan films due to the simultaneous presence of glycerol (0.5 %) and NE (25 %). In the range of glycerol concentrations employed in the current work, the glycerol concentration added did not modify the solubility of the sample, like samples with NE. The low concentration of glycerol used inside the matrix was not enough to produce significant solubility alterations. According with the FT-IR data, the increase of O—H bonds in the matrix may promote the interaction with the water molecules [29]. Consequently, the new interactions between chitosan groups with the hydrophilic groups of the plasticizer and the extract resulted in a polymer with a very low solubility of only 1.26 %. The fact that the film has such low solubility makes it interesting for application on foods with high moisture content such as cheese, meat, vegetables, or fruits. Likewise, an increase in the solubility of chitosan-based films with the addition of extracts of *Pistacia terebinthus* was observed [7]. The same behaviour was observed when tea polyphenols were added to chitosan films [30].

Due to the composite formulations (glycerol/chitosan ratio) and the hydrophilic properties of these components, the moisture content may vary depending on the composition [31]. The estimated EMC values ranged from 0.53 to 2.76 %. Data were fitted using a natural logarithmic equation to obtain better fitted, as recommended by the Box-Cox plot. The F-value of 42.92 and the p-value of 0.0003 indicated that the model was significant. The p-values showed that the linear effect of glycerol (A) and the nettle extract content (B) had a significant effect on the EMC property. The F-values showed that glycerol had a high effect on the moisture content property (F-value = 76.70). The fit statistics values indicated a r^2 value of 0.93. The predicted r^2 value of 0.85 and the adjusted r^2 value of 0.91 were in reasonable agreement and the adequate precision was 16.66.

Eq. (2) shows the EMC values of the chitosan films as a function of glycerol and NE concentration.

$$Ln\ (EMC)\ (\%) = -0.064 + 0.961 \cdot Glycerol\ (\%) - 0.003 \cdot NE\ (\%) \quad (2)$$

Fig. 3.II shows the prediction of the model for EMC given by Eq. (2). According to the data, glycerol at 0.5 % (w/w) in the film allowed the highest EMC value. This is because glycerol is a hydrophilic plasticizer. Therefore, films with higher concentrations can absorb more water into their matrix [32]. Unlike the presence of NE produced a decrease in this parameter, even the presence of hydrophilic compounds. SEM images showed that the presence of NE produced packing of the structure, having a more closed and compact matrix. This dense structure hindered the retention of water molecules, resulting in lower EMC values. This effect is maintained even in samples with high glycerol content (0.5 %). Besides, the phenols in the nettles formed interactions with the -OH and $-NH_2$ groups of the chitosan. In this way, the availability of the chitosan functional group to interact with water is limited [33].

The main purpose of a packaging film is to prevent moisture from being transferred from the environment to the food. Hence, its WVP should be as low as feasible [30]. The WVP values for the chitosan films ranged from $2.22 \cdot 10^{-11}$ to $5.64 \cdot 10^{-11}$ g/m·s·Pa. Data were well fitted to a linear model. The F-value of the model was 3.30 and the p-value was 0.1078, meaning the model was not significant. Note that the p-values of the model terms indicated that only glycerol concentration (p-value < 0.05) was significant. The fit statistics values were r^2 of 0.52. In this case,

Table 3
Antioxidant properties of chitosan (Ch) films with glycerol (Gly) and nettle extract (NE). The number in the film sample shows the % (w/w) of that compound.

Samples	DPPH (%)	ABTS (%)	Total phenolic content (mg GAE/g film sample)
Ch_Gly0	0.00 ± 0.25[a]	10.38 ± 4.37[a]	0.00 ± 0.01[a]
Ch_Gly0_NE12.5	76.11 ± 0.74[b]	92.32 ± 1.49[b]	0.12 ± 0.09[b]
Ch_Gly0_NE25	95.48 ± 0.14[c]	98.71 ± 0.00[b]	0.67 ± 0.07[c]
Ch_Gly0.25	0.33 ± 1.48[a]	11.61 ± 10.89[a]	0.00 ± 0.01[a]
Ch_Gly0.25_NE12.5	92.20 ± 0.38[d]	98.46 ± 0.11[b]	0.63 ± 0.05[c]
Ch_Gly0.25_NE25	95.48 ± 0.14[c]	97.24 ± 1.15[b]	1.57 ± 0.06[d]
Ch_Gly0.5	0.66 ± 2.75[a]	15.17 ± 6.14[a]	0.00 ± 0.04[a]
Ch_Gly0.5_ NE12.5	84.65 ± 1.14[e]	98.71 ± 0.00[b]	0.64 ± 0.17[c]
Ch_Gly0.5_ NE25	95.40 ± 0.14[cd]	98.34 ± 0.00[b]	1.52 ± 0.06[d]

Values are expressed as mean ± standard deviation (SD).
Different letters in the same column indicate significant differences ($p < 0.05$).

the values of predicted and adjusted r^2 were not in reasonable agreement, and adequate precision (4.06) indicated an adequate signal.

The WVP property of the chitosan films samples could be predicted using Eq. (3). The prediction of the model is shown in Fig. 3.III.

$$\text{WVP}\ (\text{g/m·s·Pa}) = 3.18{\cdot}10^{-11} + 3.56{\cdot}10^{-11}{\cdot}Glycerol\ (\%) - 9.06{\cdot}10^{-14}{\cdot}NE\ (\%) \quad (3)$$

The addition of NE showed no significant differences (p-value > 0.05) in WVP values compared to pure chitosan films. A significant decrease (p-value < 0.05) in WVP values was only observed when the NE concentration was 25 % and no glycerol was used. This could be attributed to the fact that the interactions between chitosan and NE could reduce the availability of hydrophilic groups in chitosan and decrease their interactions with water [34]. On the other hand, the addition of glycerol in the rest of the samples has no significant effect on this property. Except when it was added to the pure chitosan matrix with a concentration of 0.5 % where a significant increase (p-value < 0.05) in the permeability of pure chitosan films occurs. This is explained by the fact that the glycerol is a hydrophilic molecule that can be inserted between adjacent polymer chains. In this way, it decreases intermolecular attractions and facilitates the migration of water vapor molecules, increasing permeability [35]. In addition, it should be noted that the permeability of a film depends on its chemical structure, morphology, nature of permeant and temperature of the environment [36].

3.4. Evaluation of antioxidant properties

The antioxidant capacity of the films was evaluated by three methods: DPPH, ABTS, and total phenolic content (Table 3). Films enriched with NE showed a strong free-radical scavenging activity with values ranging between 76.11 % and 95.48 % for DPPH. Data were fitted to a square root model as recommended by the Box-Cox plot. The F-value of 659.66 and p-value < 0.0001 indicated that the model was significant. The p-values showed that the NE concentration (B) and the quadratic effect of NE (B^2) had a significant response on the DPPH values of the films. On the other hand, the F-values showed that the NE content (F-value = 1495.85) and the quadratic effect of NE content (F-value = 664.73) were the two factors that had the greatest impact on this property. The glycerol-NE interaction (F-value = 3.52), the glycerol concentration (F-value = 0.70) and the quadratic effect of glycerol content (F-value = 2.88) demonstrated that had negligible influence on

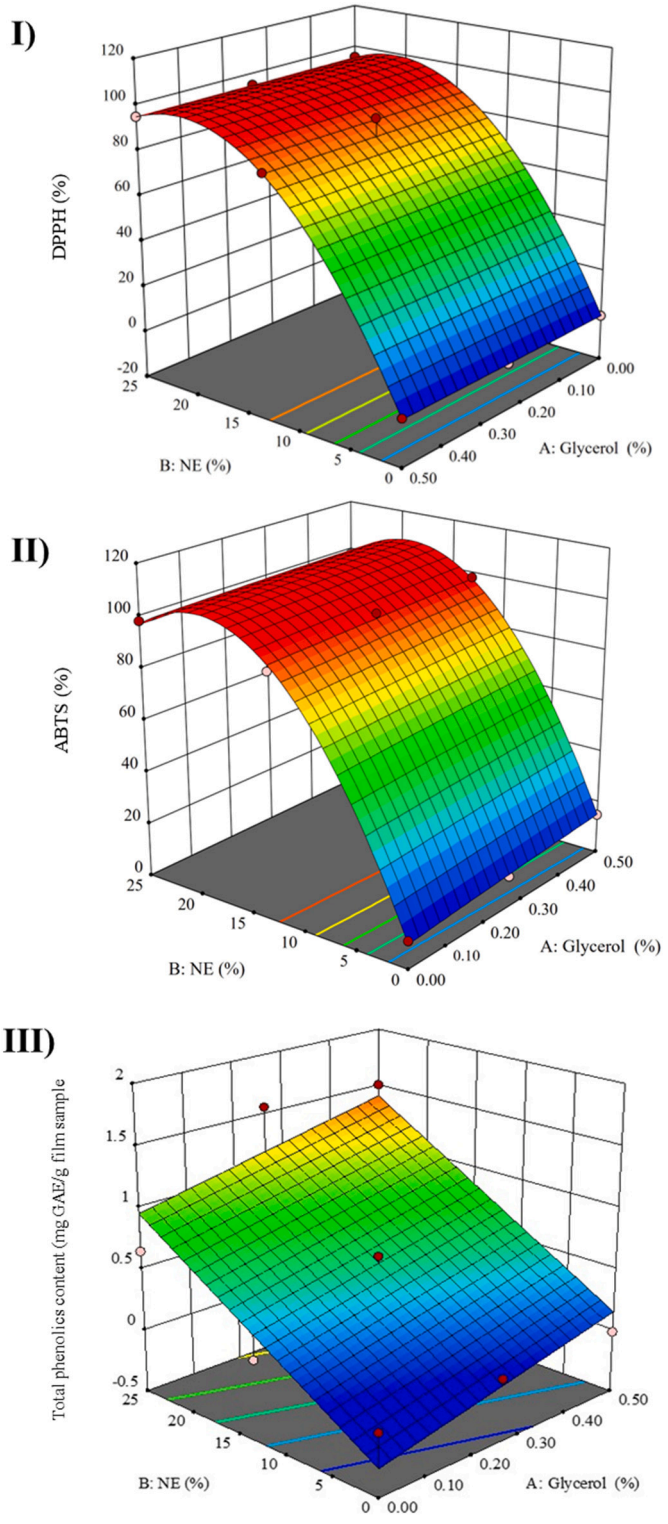

Fig. 4. Prediction of the models for antioxidant properties: I) DPPH (%), II) ABTS and III) total phenolics content (mg GAE/g film sample). NE is nettle extract.

the scavenging property (Table S3). The fit statistics values indicated r^2 of 0.99. The predicted r^2 value of 0.99 and the adjusted r^2 value of 0.99 were in reasonable agreement. The model showed adequate precision with a value of 55.01 (Table S4).

Eq. (4) forecasts the DPPH values of the chitosan films as a function of glycerol (A) and NE content (B). Fig. 4.I shows the calculated

Table 4
Optical properties of the chitosan (Ch) films with glycerol (Gly) and nettle extract (NE). The number in the film sample shows the % (w/w) of that compound.

Film samples	UV-C 200–280 nm (%T)	UV-B 280–315 nm (%T)	UV-A 315–400 nm (%T)	Transparency	Opacity
Ch_Gly0	17.20 ± 11.34	34.76 ± 22.57	47.32 ± 24.89	45.37	4.11
Ch_Gly0_NE12.5	0.52 ± 0.22	1.82 ± 0.65	11.43 ± 1.73	37.19	6.78
Ch_Gly0_NE25	0.01 ± 0.01	0.05 ± 0.03	2.46 ± 0.43	38.10	9.54
Ch_Gly0.25	20.19 ± 0.40	42.87 ± 0.74	58.31 ± 0.13	41.38	2.35
Ch_Gly0.25_NE12.5	0.21 ± 0.09	0.79 ± 0.29	9.97 ± 1.62	40.24	6.53
Ch_Gly0.25_NE25	0.01 ± 0.01	0.04 ± 0.02	3.60 ± 0.60	42.07	9.18
Ch_Gly0.5	15.58 ± 0.27	32.58 ± 0.59	51.01 ± 0.07	37.32	2.11
Ch_Gly0.5_ NE12.5	0.18 ± 0.11	0.74 ± 0.38	8.53 ± 1.77	36.45	7.48
Ch_Gly0.5_ NE25	0.00 ± 0.00	0.01 ± 0.00	2.55 ± 0.20	34.50	8.42

%T is percentage of transmittance. Values are expressed as mean ± standard deviation.

dependence of the DPPH given by Eq. (4).

$$\sqrt{\text{DPPH}} = -0.04 + 3.83 \cdot Glycerol\,(\%) + 1.03 \cdot NE\,(\%) - 0.06 \cdot Glycerol\,(\%) \cdot NE\,(\%) - 4.27 \cdot Glycerol^2\,(\%) - 0.02 \cdot NE^2\,(\%) \quad (4)$$

The DPPH values of the films are drastically increased when nettle extract is added to the composition, which has already been mentioned in the statistical commentary. From these results, it can be determined that the antioxidant capacity of the films enhanced once NE was added [37].

The ABTS values of the samples ranged from 10.38 to 98.71 % (Table 3). The F-value of the model was 639.48, while the p-value was <0.05, which means that the model was significant. The p-values of the NE concentration (B) and the quadratic effect of NE (B^2) were the terms that had a significant response on this antioxidant property. Regarding the F-values, the NE content (F-value = 917.51) and the quadratic effect of NE content (F-value = 753.23) were by far the values that most affected the ABTS values. In terms of fit statistics values, the r^2 was 0.99, whereas the predicted r^2 (0.9911) and the adjusted r^2 (0.9975) were in total agreement. The adequate precision of the model was >4, namely with a value of 51.45

Eq. (5) estimates the ABTS response as a function of glycerol and NE concentration on the chitosan films. Fig. 4.II shows the prediction of the model.

$$\text{ABTS} = 9.24 + 13.68 \cdot Glycerol\,(\%) + 10.13 \cdot NE\,(\%) - 0.41 \cdot Glycerol\,(\%) \cdot NE\,(\%) - 2.64 \cdot Glycerol^2\,(\%) - 0.26 \cdot NE^2\,(\%) \quad (5)$$

In Fig. 4.II, the significant effect of NE on ABTS values can be observed. In the pure chitosan film, the ABTS value was 10.38 %, while the addition of NE at 12.5 % already produced an increase to 92.32 %.

The TPC values of the film samples ranged from 0 to 1.57 mg GAE/g film. Data were fitted to a square root model as recommended the Box-Cox plot. The F-value of the model was 40.81 and the p-value was <0.05, which confirms that the model was significant. Only the NE concentration (p-value 0.0001) was a significant term. Regarding the F-value, the NE (F-value = 76.81) was the factor that most affected this property. The r^2 was 0.93, the predicted r^2 0.83 and the adjusted r^2 was 0.90. As there is no difference >0.20 between the predicted and adjusted r^2, it is considered that the values are in reasonable agreement. The adequate precision of the model was 15.49.

Eq. (6) predicts the TPC response on chitosan films as a function of glycerol and NE concentration.

$$\sqrt{\text{TPC}} = -0.10 + 0.55 \cdot Glycerol\,(\%) + 0.04 \cdot NE\,(\%) \quad (6)$$

Fig. 4.III shows the prediction of the model for TPC. Significant differences ($p < 0.05$) between the pure films and the films with NE in their composition were observed. The observed increase in TPC in NE-enriched films provides further evidence of the phenolic richness of the aqueous extract, consistent with previous reports [15]. Nettle extract is a good source of phenolic components such as ursolic acid, quercetin, and phenolic acids [38]. As well, this behaviour was in agreement with other reported results such as chitosan films with the addition of *Piper betle* L. leaf extract [39], tea tree essential oil [22] or jujube leaf extract [40].

3.5. Evaluation of the spectral properties

The UV-barrier characteristics of nettle extract-chitosan films were assessed using transmittance values in the UV region, while the color and opacity of the films were determined based on transmittance values

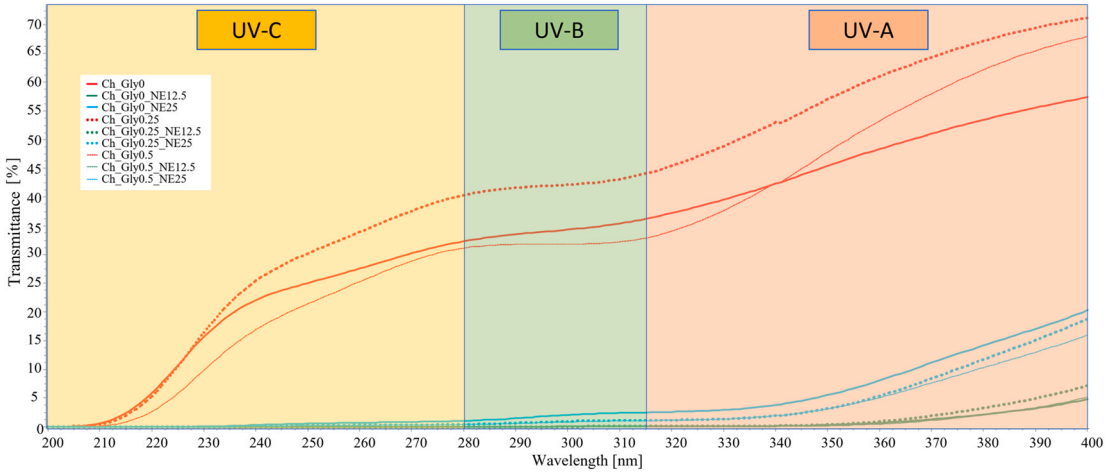

Fig. 5. UV Spectra profile of chitosan (Ch) films at different concentration of glycerol (Gly) (0, 0.25, 0.5 %) and nettle extract (NE) (0, 12.5, 25 %).

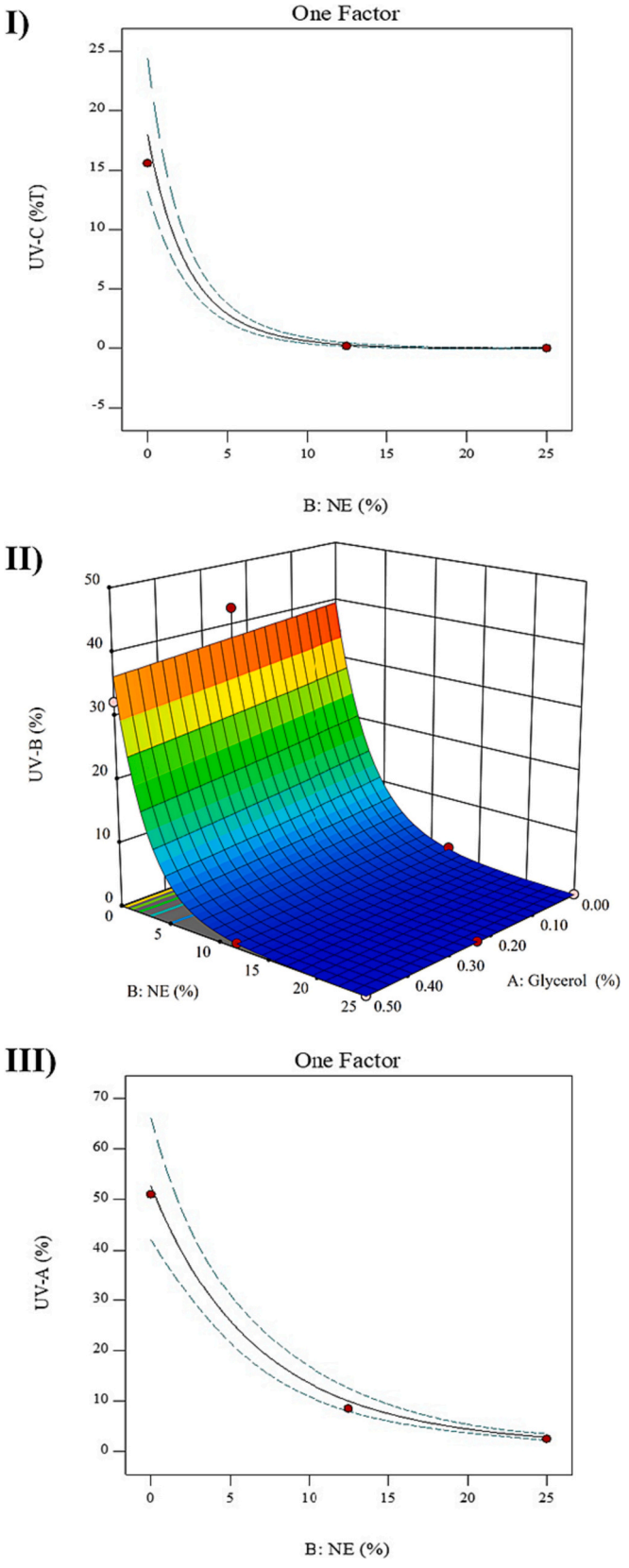

Fig. 6. Prediction of the models for the UV transmittance: I) UV-C (%T), II) UV-B (%T), III) UV-A (%T). NE is nettle extract.

in the visible region. Table 4 shows the average percentage of transmittance (%T) of the Ch_NE films in the UV-C (200–280 nm), UV-B (280–315 m) and UV-A (315–400 nm) regions. The UV spectrum of the films is shown in Fig. 5. Ch_NE films showed %T values in the UV-C region ranging from 0.01 to 20.19 %. As recommended by Box-Cox plot, data of UV-C barrier properties were fitted using a logarithmic equation to obtain better fitted. The F-value of the model was 269.95 and the p-value<0.0001, which means that the model was significant. The p-values indicated that the linear and quadratic effects of NE concentration (B and B^2) were the only significant terms ($p < 0.05$) with effect as UV-C barrier. The presence of glycerol did not influence the transmission of UV-C (Table S5).

The fit statistics results indicated r^2 of 0.98. The adjusted r^2 was 0.98 and the predicted r^2 was 0.97. Therefore, it is considered that there is a reasonable agreement. The model showed adequate signal (32.49) being >4 (Table S6). Eq. (7) predicts the UV-C response in terms of actual factors of glycerol and NE concentration and Fig. 6.I shows the calculated dependence of UV-C property on the NE concentration in chitosan films.

$$\mathrm{Ln}\,(\mathrm{UV}-\mathrm{C})\,(\%) = 1.249 - 0.173{\cdot}NE\,(\%) + 0.003{\cdot}NE^2\,(\%) \quad (7)$$

The UV-B transmittance showed values from 0.01 to 42.87 %. In this case, the F-value of the model was 362.39, and the p-value was <0.0001. Therefore, the model was significant. All terms were significant since all p-values were <0.05. Regarding the F-values, the linear effect of NE was the term with the highest value, making it the most influential. In terms of the fit statistics results, these indicated an r^2 of 0.99, a predicted r^2 of 0.98, and an adjusted r^2 of 0.99. The model was in reasonable agreement and with an adequate precision of 44.70. Eq. (8) forecasts the UV-B response based on the concentrations of glycerol and NE and the calculated dependence of UV-B property in chitosan films is shown in Fig. 6.II.

$$\mathrm{Ln}\,(\mathrm{UV}-\mathrm{B})\,(\%) = 1.58\text{–}0.07{\cdot}Glycerol\,(\%) - 0.11{\cdot}NE\,(\%) - 0.05{\cdot}Glycerol\,(\%){\cdot}NE\,(\%) \quad (8)$$

Values for UV-A property ranged from 2.46 to 58.31 %. The mathematical model was significant since its p-value was <0.0001 and the F-value was 250.01. The term that was found to be significant was the linear effect of NE (p-value ≤ 0.0001). The terms with higher F-value were linear NE (F-value = 374.02) and the quadratic effect of NE (F-value = 3.19). The fit statistics results indicated a r^2 of 0.98. The adjusted r^2 (0.98) and the predicted r^2 (0.97) were found with a difference of <0.20. Therefore, they were in reasonable agreement. A ratio >4 indicates adequate model discrimination and in this case was of 31.52.

Fig. 6.III depicts the calculated dependence of the UV-A transmittance on the glycerol and NE concentrations in the chitosan films and Eq. (9) predicts the UV-A response.

$$\mathrm{Ln}\,(\mathrm{UV}-\mathrm{A})\,(\%) = 1.7161 - 0.0646{\cdot}NE\,(\%) + 0.0005{\cdot}NE^2\,(\%) \quad (9)$$

These results show that the addition of NE exerted a strong decrease in UV light transmittance compared with pure chitosan film. The lowest transmission through films was observed for the highest concentration of extract. These results confirmed that chitosan film containing NE could retard lipid oxidation induced by UV light in food systems due to barrier effect.

The transparency and opacity of the films are other important factors to be studied. The transparency of films must fulfil consumer eagerness to see food through packaging. Table 4 shows the values of transparency in pure chitosan film ranged from 37.32 to 45.37. The addition of NE to chitosan films resulted in a slightly decrease in transparency (34.50–42.07). However, the obtained mathematical model was not significant, indicating that the transparency of samples does not depend on their formulation. The F-value and p-value of the model were 2.40 and 0.1708, respectively. Being a non-significant model, none of the

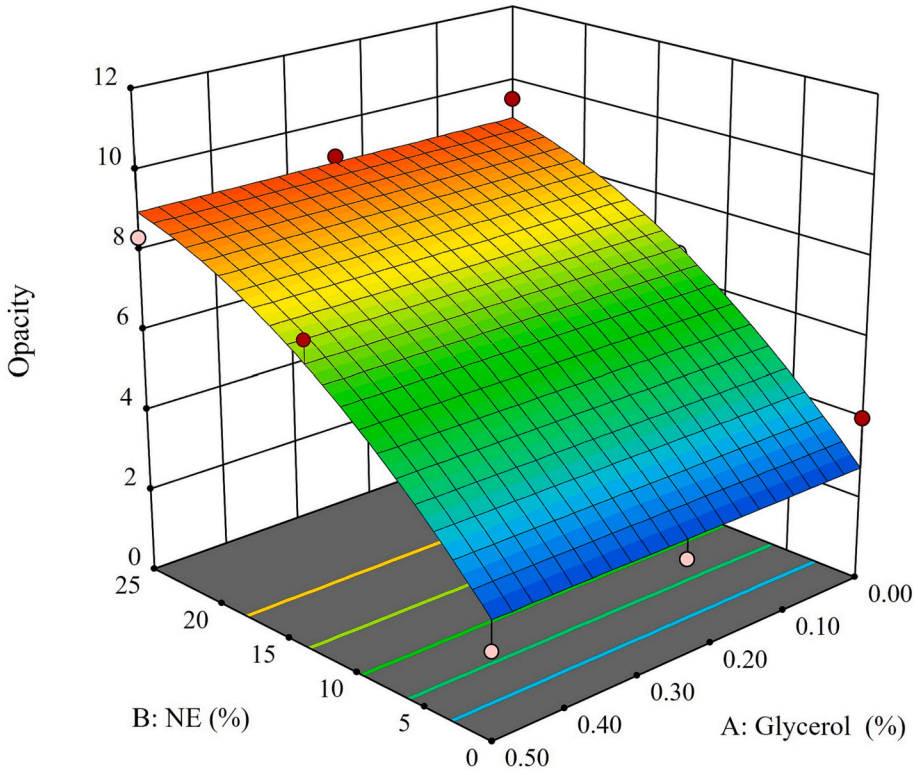

Fig. 7. Prediction of the model for the opacity of the films. NE is nettle extract.

Table 5
Color parameters of the chitosan (Ch) films with glycerol (Gly) and nettle extract (NE). The number in the film sample shows the % (w/w) of that compound.

Samples	L*	a*	b*
Ch_Gly0	90.19 ± 0.01^{a}	-0.22 ± 0.04^{c}	2.12 ± 0.19^{a}
Ch_Gly0_NE12.5	77.32 ± 1.53^{bc}	-2.10 ± 0.19^{b}	14.15 ± 1.19^{b}
Ch_Gly0_NE25	72.08 ± 0.47^{b}	-3.82 ± 0.06^{c}	26.20 ± 1.39^{c}
Ch_Gly0.25	91.28 ± 0.36^{a}	-0.28 ± 0.03^{a}	2.51 ± 0.04^{a}
Ch_Gly0.25_NE12.5	79.45 ± 1.36^{c}	-2.95 ± 0.12^{d}	15.58 ± 1.60^{b}
Ch_Gly0.25_NE25	74.69 ± 1.24^{bc}	-4.41 ± 0.12^{e}	24.19 ± 1.38^{c}
Ch_Gly0.5	91.39 ± 0.52^{a}	-0.53 ± 0.06^{a}	3.23 ± 0.08^{a}
Ch_Gly0.5_ NE12.5	75.22 ± 3.56^{bc}	-2.53 ± 0.15^{f}	16.13 ± 0.98^{b}
Ch_Gly0.5_ NE25	72.59 ± 0.69^{b}	-4.33 ± 0.02^{e}	26.18 ± 0.46^{c}

L*, lightness: black = 0 and white = 100; a*, green = −a* and red = +a*; b*, blue = −b* and yellow = +b*.
Values are expressed as mean ± standard deviation.
Different letters in the same column indicate significant differences ($p < 0.05$).

terms involved had a $p < 0.05$ (Table S5). The fit statistics results indicated a r^2 of 0.44. The adjusted r^2 and predicted r^2 were 0.26 and −0.23, respectively. The adequate precision was 4.34 (Table S6). Based on this result, it can be inferred that the model lacks statistical reliability and should not be utilized.

The values of opacity increased when NE was added to the matrix. In this case, the mathematical model was significant, showing an F-value of 39.29 and a p-value of 0.0003. The p-values of the terms indicated that the linear effect of NE concentration was the only significant term (p-value = 0.0001). The same result was observed regarding the F-value of linear NE, where this term had the highest F-value (77.28), indicating that NE had great impact on the opacity. Regarding the fit statistics values, r^2 was 0.92 and the predicted r^2 (0.84) was in reasonable agreement with the adjusted r^2 (0.90). The adequate precision of the model was 14.05. In terms of the real factor of glycerol and NE concentration in films, Eq. (10) forecasts the opacity response. Fig. 7 shows the prediction of the model for the opacity of the films.

$$\text{Opacity} = 3.58 - 1.61 \cdot Glycerol\ (\%) + 0.24 \cdot NE\ (\%) \quad (10)$$

Likewise, the increase in opacity can be attributed to the higher saturated color of NE. In addition, when the NE was added to the matrix, the structure tended to be more off white compared to the pure chitosan film. This could be due to the hydrophilicity of the polyphenolic compounds present in NE [41].

The CIE coordinate of the Ch_NE films is shown in Table 5. Lightness (L*) varied from 72.08 to 91.39. The addition of NE to the chitosan films had a significant effect ($p < 0.05$), producing a decrease in L* values. This result is interpreted as film darkening upon the application of the plant extract. The F-value of the model was 58.37 and the p-value was 0.0034, implying the model was significant. According to the p-values, only the linear and quadratic effects of NE concentration were significant (p-value < 0.05). Regarding the F-values, the terms that affected the Lightness the most were the linear effect of NE (F-value = 109.28) and the quadratic effect of NE (F-value = 24.42) (Table S5). The r^2 was 0.98, whereas the adjusted r^2 was 0.97 and the predicted r^2 was 0.88, respectively. This indicates that the model is in reasonable agreement as well as having an adequate precision of 18.25 (Table S6). Eq. (11) predicts the L* values of the chitosan films and the prediction of the model is shown in Fig. 8.I.

$$L^{*} = 90.17 + 16.49 \cdot Glycerol\ (\%) - 1.45 \cdot NE\ (\%) - 0.05 \cdot Glycerol\ (\%) \cdot NE\ (\%) - 32.13 \cdot Glycerol^{2}\ (\%) + 0.03 \cdot NE^{2}\ (\%) \quad (11)$$

As for the values of a*, these were in the range from −0.22 to −4.41. The addition of NE produced a significant decrease ($p < 0.05$) of a* values, which means that the films tend to greenness, clearly produced by the color of NE. The mathematical model obtained was also significant, F-value of 134.29 and p-value of $1.04 \cdot 10^{-5}$. The only term with a significant p-value was the NE concentration (p-value = $3.40 \cdot 10^{-6}$) and it was the term with the highest effect (F-value = 265.51) in the a* property. The r^2 was 0.97, the adjusted r^2 was 0.97 and the predicted r^2

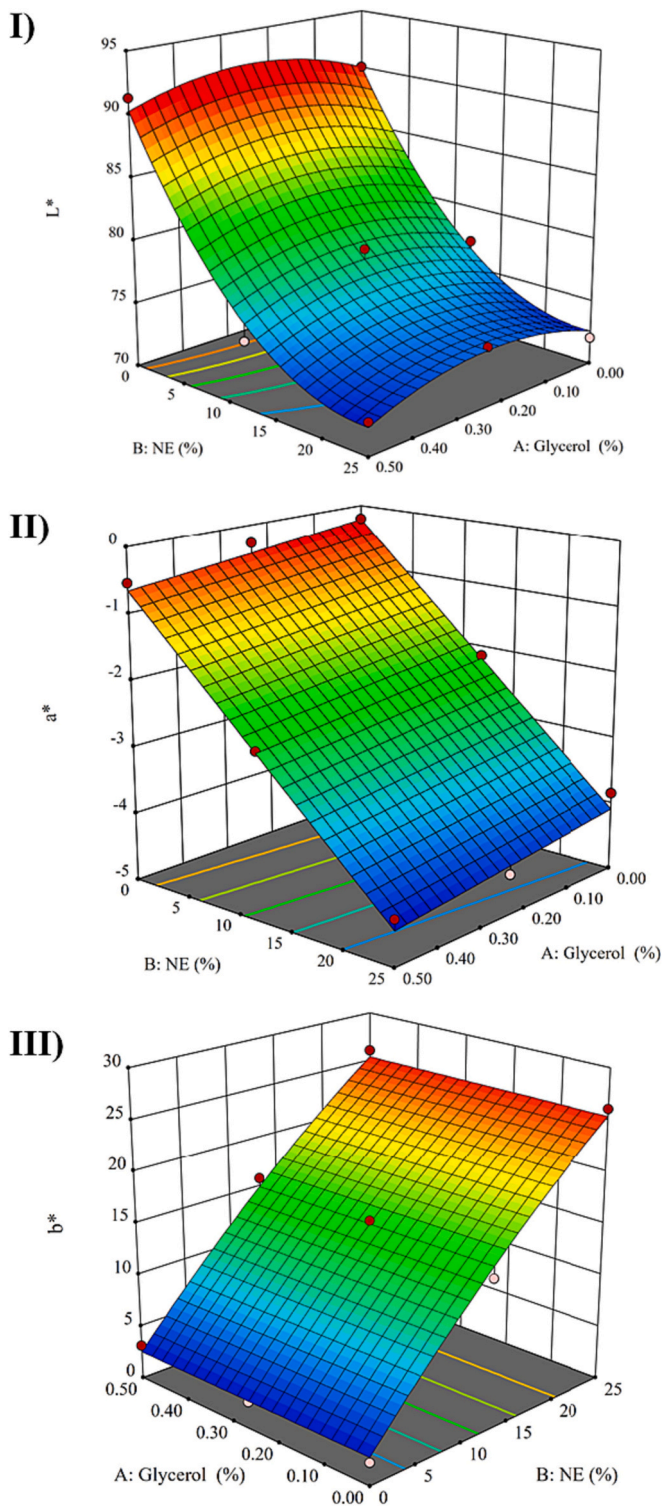

Fig. 8. Prediction of the models for the CIE coordinates: I) L*, II) a* and III) b*. NE is nettle extract.

was 0.96, indicating reasonable agreement. The model was in adequate precision, 25.52. Fig. 8.II depicts the prediction of the model for the a* parameter of the chitosan films based on Eq. (12).

$$a^* = -0.22 - 0.82 \cdot Glycerol\ (\%) - 0.15 \cdot NE\ (\%) \quad (12)$$

The films produced with incorporation of NE resulted in a tendency toward yellowness, with values for b* ranged from 2.12 to 26.20. The mathematical model had an F-value of 347.01 and a p-value of $6.29 \cdot 10^{-7}$, indicating that it was significant. As before, the term with a p-value < 0.05 and the greatest F-value (692.64) was the linear effect of NE. In terms of the fit statistics values, r^2 was 0.99 and the predicted r^2 (0.98) and the adjusted r^2 (0.98) were in totally reasonable agreement. The adequate precision of the equation was 38.87.

The prediction of the model for the b* parameter of the chitosan films based on Eq. (13) is shown in Fig. 8.III.

$$b^* = 2.51 + 2.04 \cdot Glycerol\ (\%) + 0.91 \cdot NE\ (\%) \quad (13)$$

Regarding the CIE coordinate properties, the same behaviour of the chitosan films was observed when other extracts were added, such as green tea extract [36] or spirulina [42].

4. Conclusions

Incorporation of NE into the chitosan matrix was successfully carried out to obtain antioxidant films. The results obtained showed that the incorporation of NE allowed obtaining chitosan films with antioxidant properties containing TPC up to 1.57 mg GAE/g film and showing a high ABTS and DPPH scavenging activity up to 98 %. Furthermore, the antioxidant capacity produced by the extract was reinforced by the high UV barrier observed in the NE films. The NE-enriched films showed UV-C and UV-B transmittance values close to zero, and up to 11 % in the UV-A region. However, when NE was added to the matrix, the structure tended to become more yellowish and opaquer. Although, a sufficiently transparent film was still obtained that would allow to see the packaged food. Furthermore, these films with NE boast a total UV barrier and low water solubility. The inherent biodegradability is also a strong advantage of the developed active film.

CRediT authorship contribution statement

All authors discussed the results and contributed to the final manuscript.

Declaration of competing interest

The authors have no conflict of interest to declare.

Acknowledgements

The authors appreciate the funding support of Xunta de Galicia, within the postdoctoral fellowship granted to Patricia Cazón Díaz (No. ED481B-2021-040). We acknowledge the use of RIAIDT-USC analytical facilities.

Appendix A. Supplementary data

Supplementary data to this article can be found online at https://doi.org/10.1016/j.ijbiomac.2023.127318.

References

[1] S. Dehghani, S.V. Hosseini, J.M. Regenstein, Edible films and coatings in seafood preservation: a review, Food Chem. 240 (2018) 505–513, https://doi.org/10.1016/j.foodchem.2017.07.034.

[2] M.Z. Elsabee, E.S. Abdou, Chitosan based edible films and coatings: a review, Mater. Sci. Eng. C 33 (2013) 1819–1841, https://doi.org/10.1016/j.msec.2013.01.010.

[3] A.P. Lunkov, A.V. Ilyina, V.P. Varlamov, Antioxidant, antimicrobial, and fungicidal properties of chitosan based films (review), Appl. Biochem. Microbiol. 54 (2018) 449–458, https://doi.org/10.1134/S0003683818050125.

[4] M. Mujtaba, R.E. Morsi, G. Kerch, M.Z. Elsabee, M. Kaya, J. Labidi, K.M. Khawar, Current advancements in chitosan-based film production for food technology; a review, Int. J. Biol. Macromol. 121 (2019) 889–904, https://doi.org/10.1016/j.ijbiomac.2018.10.109.

[5] Y. Flores, C.J. Pelegrín, M. Ramos, A. Jiménez, M.C. Garrigós, Use of herbs and their bioactive compounds in active food packaging, in: Aromat. Herbs Food

Bioact. Compd. Process. Appl, 2021, pp. 323–365, https://doi.org/10.1016/B978-0-12-822716-9.00009-3.
[6] A. Valdés, A.C. Mellinas, M. Ramos, N. Burgos, A. Jiménez, M.C. Garrigós, Use of herbs, spices and their bioactive compounds in active food packaging, RSC Adv. 5 (2015) 40324–40335, https://doi.org/10.1039/c4ra17286h.
[7] M. Kaya, S. Khadem, Y.S. Cakmak, M. Mujtaba, S. Ilk, L. Akyuz, A.M. Salaberria, J. Labidi, A.H. Abdulqadir, E. Deligöz, Antioxidative and antimicrobial edible chitosan films blended with stem, leaf and seed extracts of Pistacia terebinthus for active food packaging, RSC Adv. 8 (2018) 3941–3950, https://doi.org/10.1039/C7RA12070B.
[8] M. Flórez, P. Cazón, M. Vázquez, Active packaging film of chitosan and Santalum album essential oil: characterization and application as butter sachet to retard lipid oxidation, Food Packag. Shelf Life 34 (2022), 100938, https://doi.org/10.1016/j.fpsl.2022.100938.
[9] R. Chollakup, S. Pongburoos, W. Boonsong, N. Khanoonkon, Antioxidant and antibacterial activities of cassava starch and whey protein blend films containing rambutan peel extract and cinnamon oil for active packaging, LWT Food Sci. Technol. 130 (2020), 109573, https://doi.org/10.1016/j.lwt.2020.109573.
[10] M. Mzid, S. Ben Khedir, S. Bardaa, Z. Sahnoun, T. Rebai, Chemical composition, phytochemical constituents, antioxidant and anti-inflammatory activities of Urtica urens L. leaves, Arch. Physiol. Biochem. 123 (2017) 93–104, https://doi.org/10.1080/13813455.2016.1255899.
[11] A.P. Simopoulos, Essential fatty acids in health and chronic diseases, Forum Nutr. 56 (2003) 67–70.
[12] S. Đurović, B. Pavlić, S. Šorgić, S. Popov, S. Savić, M. Pertonijević, M. Radojković, A. Cvetanović, Z. Zeković, Chemical composition of stinging nettle leaves obtained by different analytical approaches, J. Funct. Foods 32 (2017) 18–26, https://doi.org/10.1016/j.jff.2017.02.019.
[13] M. Repajić, E. Cegledi, V. Kruk, S. Pedisić, F. Çinar, D.B. Kovačević, I. Žutić, V. Dragović-Uzelac, Accelerated solvent extraction as a green tool for the recovery of polyphenols and pigments fromwild nettle leaves, Processes. 8 (2020) 1–19, https://doi.org/10.3390/pr8070803.
[14] A. Rita, G. Costa, A. Figueirinha, J. Liberal, J.A.V. Prior, M. Celeste, M. Teresa, M. Teresa, Urtica spp.: phenolic composition, safety, antioxidant and anti-inflammatory activities, Food Res. Int. 99 (2017) 485–494, https://doi.org/10.1016/j.foodres.2017.06.008.
[15] M. Flórez, P. Cazón, M. Vázquez, Antioxidant extracts of nettle (Urtica dioica) leaves: evaluation of extraction techniques and solvents, Molecules. 27 (2022) 6015, https://doi.org/10.3390/molecules27186015.
[16] H. Almasi, M. Zandi, S. Beigzadeh, S. Haghju, N. Mehrnow, Chitosan films incorporated with nettle (Urtica dioica L.) extract-loaded nanoliposomes: II. Antioxidant activity and release properties, J. Microencapsul. 33 (2016) 449–459, https://doi.org/10.1080/02652048.2016.1208295.
[17] F. Bigi, H. Haghighi, H.W. Siesler, F. Licciardello, A. Pulvirenti, Characterization of chitosan-hydroxypropyl methylcellulose blend films enriched with nettle or sage leaf extract for active food packaging applications, Food Hydrocoll. 120 (2021), 106979, https://doi.org/10.1016/J.FOODHYD.2021.106979.
[18] P. Cazón, M. Vázquez, G. Velazquez, Composite films with UV-barrier properties based on bacterial cellulose combined with chitosan and poly(vinyl alcohol): study of puncture and water interaction properties, Biomacromolecules. 20 (2019) 2084–2095, https://doi.org/10.1021/acs.biomac.9b00317.
[19] P. Cazón, E. Morales-Sanchez, G. Velazquez, M. Vázquez, Measurement of the water vapor permeability of chitosan films: a laboratory experiment on food packaging materials, J. Chem. Educ. 99 (2022) 2403–2408, https://doi.org/10.1021/acs.jchemed.2c00449.
[20] C. Bottesini, S. Paolella, F. Lambertini, G. Galaverna, T. Tedeschi, A. Dossena, R. Marchelli, S. Sforza, Antioxidant capacity of water soluble extracts from Parmigiano-Reggiano cheese, Int. J. Food Sci. Nutr. 64 (2013) 953–958, https://doi.org/10.3109/09637486.2013.821696.
[21] J. Rutkowska, A. Antoniewska, M. Martinez-Pineda, A. Nawirska-Olszańska, A. Zbikowska, D. Baranowski, Black chokeberry fruit polyphenols: a valuable addition to reduce lipid oxidation of muffins containing xylitol, Antioxidants. 9 (2020) 394, https://doi.org/10.3390/antiox9050394.
[22] P. Cazón, A. Antoniewska, J. Rutkowska, M. Vázquez, Evaluation of easy-removing antioxidant films of chitosan with Melaleuca alternifolia oil, Int. J. Biol. Macromol. 186 (2021) 365–376, https://doi.org/10.1016/J.IJBIOMAC.2021.07.035.
[23] S. Haghju, S. Beigzadeh, H. Almasi, H. Hamishehkar, Chitosan films incorporated with nettle (Urtica dioica L.) extract-loaded nanoliposomes: I. Physicochemical characterisation and antimicrobial properties, J. Microencapsul. 33 (2016) 438–448, https://doi.org/10.1080/02652048.2016.1208294.
[24] I. Bilican, S. Pekdemir, M.S. Onses, L. Akyuz, E.M. Altuner, B. Koc-Bilican, L. S. Zang, M. Mujtaba, P. Mulerčikas, M. Kaya, Chitosan loses innate beneficial properties after being dissolved in acetic acid: supported by detailed molecular modeling, ACS Sustain. Chem. Eng. 8 (2020) 18083–18093, https://doi.org/10.1021/acssuschemeng.0c06373.
[25] R. Priyadarshi, B. Sauraj Kumar, Y.S. Negi, Chitosan film incorporated with citric acid and glycerol as an active packaging material for extension of green chilli shelf life, Carbohydr. Polym. 195 (2018) 329–338, https://doi.org/10.1016/j.carbpol.2018.04.089.
[26] H. Schulz, M. Baranska, Identification and quantification of valuable plant substances by IR and Raman spectroscopy, Vib. Spectrosc. 43 (2007) 13–25, https://doi.org/10.1016/j.vibspec.2006.06.001.
[27] S. Rivero, L. Damonte, M.A. García, A. Pinotti, An insight into the role of glycerol in chitosan films, Food Biophys. 11 (2016) 117–127, https://doi.org/10.1007/s11483-015-9421-4.
[28] S. Mathew, M. Brahmakumar, T.E. Abraham, Microstructural imaging and characterization of the mechanical, chemical, thermal, and swelling properties of starch-chitosan blend films, Biopolymers. 82 (2007) 176–187, https://doi.org/10.1002/bip.
[29] M.A. Cerqueira, B.W.S. Souza, J.A. Teixeira, A.A. Vicente, Effect of glycerol and corn oil on physicochemical properties of polysaccharide films - a comparative study, Food Hydrocoll. 27 (2012) 175–184, https://doi.org/10.1016/j.foodhyd.2011.07.007.
[30] L. Wang, Y. Dong, H. Men, J. Tong, J. Zhou, Preparation and characterization of active films based on chitosan incorporated tea polyphenols, Food Hydrocoll. 32 (2013) 35–41, https://doi.org/10.1016/j.foodhyd.2012.11.034.
[31] M. Vázquez, G. Velazquez, P. Cazón, UV-shielding films of bacterial cellulose with glycerol and chitosan. Part 1: equilibrium moisture content and mechanical properties, CyTA J. Food 19 (2021) 105–114, https://doi.org/10.1080/19476337.2020.1870566.
[32] W. Thakhiew, S. Devahastin, S. Soponronnarit, Effects of drying methods and plasticizer concentration on some physical and mechanical properties of edible chitosan films, J. Food Eng. 99 (2010) 216–224, https://doi.org/10.1016/j.jfoodeng.2010.02.025.
[33] D. Kadam, S.S. Lele, Cross-linking effect of polyphenolic extracts of Lepidium sativum seedcake on physicochemical properties of chitosan films, Int. J. Biol. Macromol. 114 (2018) 1240–1247, https://doi.org/10.1016/j.ijbiomac.2018.04.018.
[34] L. Wang, H. Guo, J. Wang, G. Jiang, F. Du, X. Liu, Effects of Herba Lophatheri extract on the physicochemical properties and biological activities of the chitosan film, Int. J. Biol. Macromol. 133 (2019) 51–57, https://doi.org/10.1016/j.ijbiomac.2019.04.067.
[35] K. Ziani, J. Oses, V. Coma, J.I. Maté, Effect of the presence of glycerol and Tween 20 on the chemical and physical properties of films based on chitosan with different degree of deacetylation, Lwt. 41 (2008) 2159–2165, https://doi.org/10.1016/j.lwt.2007.11.023.
[36] U. Siripatrawan, B.R. Harte, Physical properties and antioxidant activity of an active film from chitosan incorporated with green tea extract, Food Hydrocoll. 24 (2010) 770–775, https://doi.org/10.1016/j.foodhyd.2010.04.003.
[37] A. Güder, H. Korkmaz, Evaluation of in-vitro antioxidant properties of hydroalcoholic solution extracts Urtica dioica L., Malva neglecta Wallr. and their mixture, Iran. J. Pharm. Res. 11 (2012) 913–923.
[38] A. Belščak-Cvitanović, D. Komes, K. Durgo, A. Vojvodić, A. Bušić, Nettle (Urtica dioica L.) extracts as functional ingredients for production of chocolates with improved bioactive composition and sensory properties, J. Food Sci. Technol. 52 (2015) 7723–7734, https://doi.org/10.1007/s13197-015-1916-y.
[39] T.T. Nguyen, N.H.T. Phan, C.D. Trinh, T. Van Tran, B.T.T. Pham, B.T.P. Quynh, T. K. Phung, Glycerol-plasticized chitosan film for the preservation of orange, J. Food Saf. 42 (2022), https://doi.org/10.1111/jfs.12943.
[40] X. Zhang, H. Lian, J. Shi, W. Meng, Y. Peng, Plant extracts such as pine nut shell, peanut shell and jujube leaf improved the antioxidant ability and gas permeability of chitosan films, Int. J. Biol. Macromol. 148 (2020) 1242–1250, https://doi.org/10.1016/j.ijbiomac.2019.11.108.
[41] A. Riaz, C. Lagnika, H. Luo, Z. Dai, M. Nie, M.M. Hashim, C. Liu, J. Song, D. Li, Chitosan-based biodegradable active food packaging film containing Chinese chive (Allium tuberosum) root extract for food application, Int. J. Biol. Macromol. 150 (2020) 595–604, https://doi.org/10.1016/j.ijbiomac.2020.02.078.
[42] R. Balti, M. Ben Mansour, N. Sayari, L. Yacoubi, L. Rabaoui, N. Brodu, A. Massé, Development and characterization of bioactive edible films from spider crab (Maja crispata) chitosan incorporated with Spirulina extract, Int. J. Biol. Macromol. 105 (2017) 1464–1472, https://doi.org/10.1016/j.ijbiomac.2017.07.046.